

Template-Directed Synthesis of Nets Based upon Octahemioctahedral Cages That Encapsulate Catalytically Active Metalloporphyrins

Zhenjie Zhang, Linping Zhang, Lukasz Wojtas, Mohamed Eddaoudi, and Michael J. Zaworotko*

Crystal data and structure refinement for porph@MOM-4	
Empirical formula	C ₉₄ H ₄₂ Cl _{18.50} Fe _{12.50} N ₄ O ₆₀ 8(C ₉ H ₃ O ₆), 12Fe, 12(H ₂ O), 0.5(C ₄₄ H ₃₆ N ₈ Fe ₁ Cl ₁₅), Cl ₆
Formula weight	3186.77
Temperature	100(2) K
Wavelength	1.54178 Å
Crystal system, space group	Cubic, Fm-3m
Unit cell dimensions	a = 26.5717(17) Å alpha = 90 deg. b = 26.5717(17) Å beta = 90 deg. c = 26.5717(17) Å gamma = 90 deg.
Volume	18761(2) Å ³
Z, Calculated density	4, 1.128 Mg/m ³
Absorption coefficient	9.178 mm ⁻¹
Crystal size	0.05 x 0.05 x 0.05 mm
Theta range for data collection	5.52 to 65.26 deg.
Reflections collected / unique	7378 / 848 [R(int) = 0.0760]
Completeness to theta = 64.53	97.2 %
Data / restraints / parameters	848 / 29 / 87
Goodness-of-fit on F ²	1.028
Final R indices [I > 2sigma(I)]	R1 = 0.0891, wR2 = 0.2543
R indices (all data)	R1 = 0.1278, wR2 = 0.2821
Largest diff. peak and hole	0.642 and -0.465 e. Å ⁻³

Crystal data and structure refinement for porph@MOM-5	
Empirical formula	C101.33 H75.50 Cl2.67 Co12.67 N5.33 O61.75 8(C ₉ H ₃ O ₆), 12Co, 12(H ₂ O), 0.66667 (C ₄₄ H ₃₆ N ₈ Cu ₁ Cl ₅), 1.75(H ₂ O)
Formula weight	3196.80
Temperature	100(2) K
Wavelength	0.40663 Å
Crystal system, space group	Cubic, Fm-3m
Unit cell dimensions	a = 26.4292(11) Å alpha = 90 deg. b = 26.4292(11) Å beta = 90 deg. c = 26.4292(11) Å gamma = 90 deg.
Volume	18460.9(13) Å ³
Z, Calculated density	4, 1.150 Mg/m ³
Absorption coefficient	0.233 mm ⁻¹
Crystal size	0.05 x 0.05 x 0.05 mm
Theta range for data collection	1.97 to 14.02 deg.
Reflections collected / unique	34737 / 871 [R(int) = 0.0873]
Completeness to theta = 64.53	98.6 %
Data / restraints / parameters	871 / 29 / 79
Goodness-of-fit on F ²	1.003
Final R indices [I > 2sigma(I)]	R1 = 0.0815, wR2 = 0.2452
R indices (all data)	R1 = 0.0997, wR2 = 0.2648
Largest diff. peak and hole	0.623 and -0.530 e. Å ⁻³

Crystal data and structure refinement for porph@MOM-6	
Empirical formula	C101.33 H72 Cl3.33 Mn12.67 N5.33 O60 8(C ₉ H ₃ O ₆), 12Mn, 12(H ₂ O), 0.666(C ₄₄ H ₃₆ N ₈ Fe1Cl ₅)
Formula weight	3138.38
Temperature	100(2) K
Wavelength	0.40663 Å
Crystal system, space group	Cubic, Fm-3m
Unit cell dimensions	a = 26.597(2) Å alpha = 90 deg. b = 26.597(2) Å beta = 90 deg. c = 26.597(2) Å gamma = 90 deg.
Volume	18816(2) Å ³
Z, Calculated density	4, 1.108 Mg/m ³
Absorption coefficient	0.173 mm ⁻¹
Crystal size	0.01 x 0.01 x 0.01 mm
Theta range for data collection	2.28 to 13.05 deg.
Reflections collected / unique	17924 / 723 [R(int) = 0.0639]
Completeness to theta = 64.53	98.0 %
Data / restraints / parameters	723 / 29 / 76
Goodness-of-fit on F ²	1.031
Final R indices [I > 2sigma(I)]	R1 = 0.0925, wR2 = 0.2352
R indices (all data)	R1 = 0.1187, wR2 = 0.2601
Largest diff. peak and hole	0.375 and -0.376 e. Å ⁻³

Crystal data and structure refinement for porph@MOM-7	
Empirical formula	C ₇₂ H ₂₄ Ni _{10.71} O ₈₁ {[8Ni 5.333(C ₉ H ₃ O ₆) 20H ₂ O] [2Ni 2.6666(C ₉ H ₃ O ₆) 4H ₂ O]}.9H ₂ O . 0.71Ni 2858.84
Formula weight	2813.55
Temperature	100(2) K
Wavelength	1.54178 Å
Crystal system, space group	Cubic, Fm-3m
Unit cell dimensions	a = 27.478(2) Å alpha = 90 deg. b = 27.478(2) Å beta = 90 deg. c = 27.478(2) Å gamma = 90 deg.
Volume	20747(3) Å ³
Z, Calculated density	4, 0.901 Mg/m ³
Absorption coefficient	1.582 mm ⁻¹
Crystal size	0.10 x 0.10 x 0.10 mm
Theta range for data collection	6.44 to 63.58 deg.
Reflections collected / unique	8168 / 888 [R(int) = 0.0923]
Completeness to theta = 64.53	96.4 %
Data / restraints / parameters	888 / 1 / 74
Goodness-of-fit on F ²	1.091
Final R indices [I>2sigma(I)]	R1 = 0.1075, wR2 = 0.2816
R indices (all data)	R1 = 0.1329, wR2 = 0.2972
Largest diff. peak and hole	0.554 and -0.463 e. Å ⁻³

Crystal data and structure refinement for porph@MOM-9	
Empirical formula	C108 H36 O91 Zn18.66 12(C ₉ H ₃ O ₆), 18Zn, 15(H ₂ O), 0.66(C ₄₄ H ₃₆ N ₈ Zn1H ₂ O)
Formula weight	4009.50
Temperature	100(2) K
Wavelength	0.40663 Å
Crystal system, space group	Orthorhombic, Cmmm
Unit cell dimensions	a = 19.653(3) Å alpha = 90 deg. b = 44.127(6) Å beta = 90 deg. c = 14.543(2) Å gamma = 90 deg.
Volume	12612(3) Å ³
Z, Calculated density	2, 1.056 Mg/m ³
Absorption coefficient	0.361 mm ⁻¹
Crystal size	0.10 x 0.08 x 0.08 mm
Theta range for data collection	1.19 to 13.05 deg.
Reflections collected / unique	39524 / 4753 [R(int) = 0.0720]
Completeness to theta = 64.53	95.8 %
Data / restraints / parameters	4753 / 288 / 284
Goodness-of-fit on F ²	1.072
Final R indices [I > 2sigma(I)]	R1 = 0.1241, wR2 = 0.3302
R indices (all data)	R1 = 0.1357, wR2 = 0.3413
Largest diff. peak and hole	1.061 and -1.579e. Å ⁻³

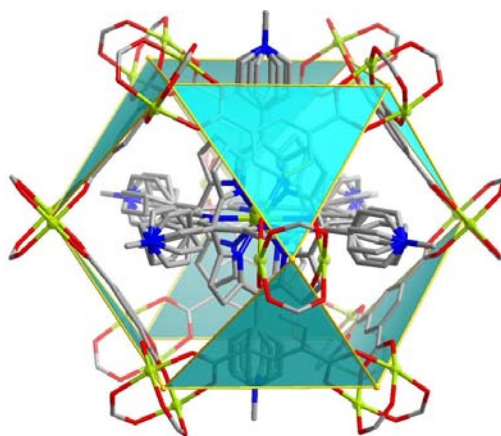


Figure S1. A TMPyP molecule appearing in three positions.

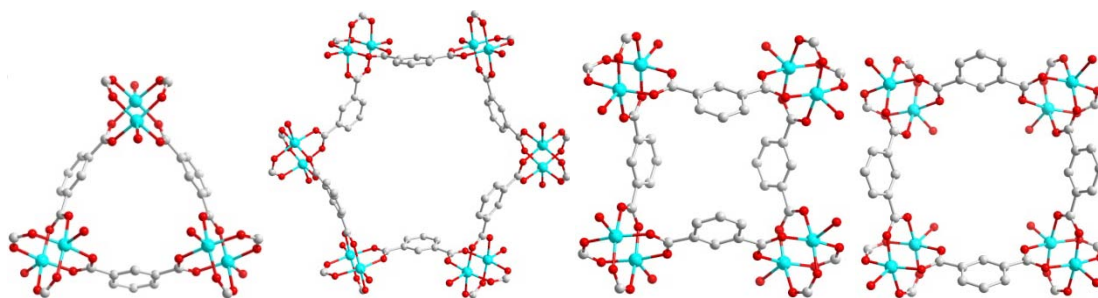


Figure S2. (From left to right) Triangle nSBU, hexagon nSBU, 1,3-alternate square nSBU and cone square nSBU.

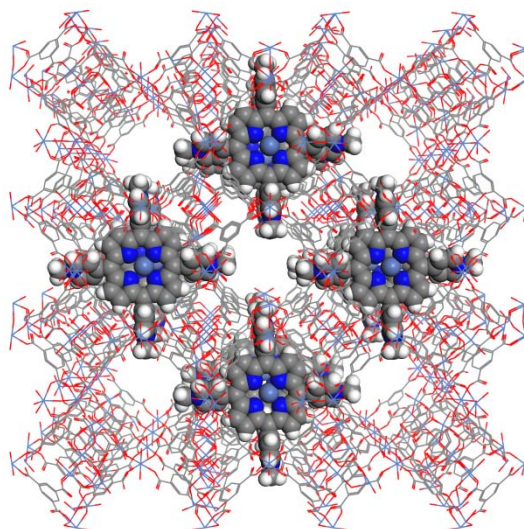


Figure S3. Projection of the structure of **porph@MOM-7** along the *a* axis and porphyrins molecules are locating in the octahemioctahedral cages.

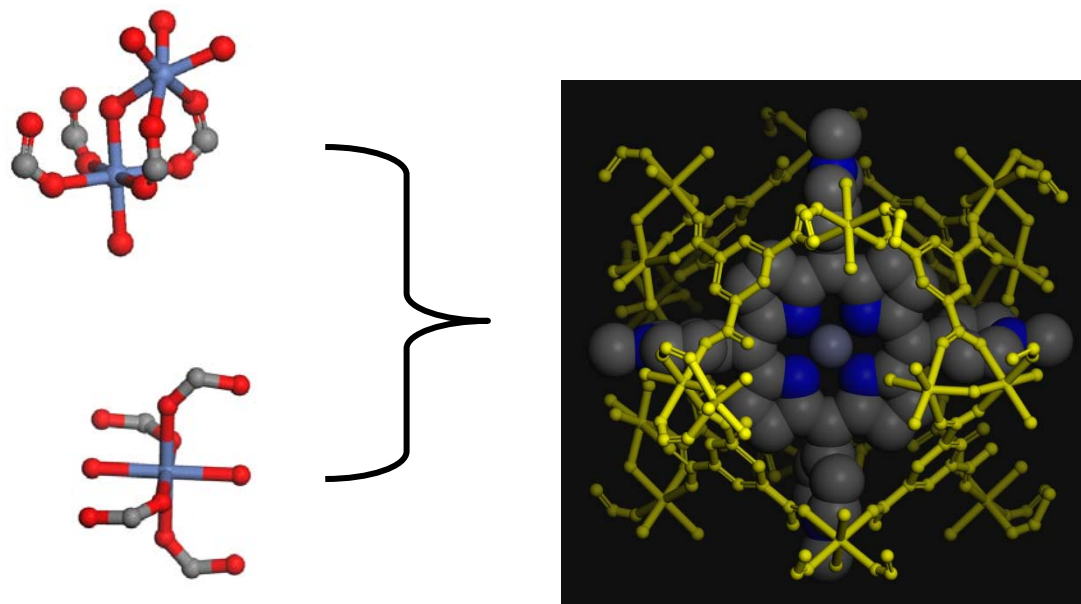


Figure S4. An illustration of the cavity in **porph@MOM-7** that contains porphyrin molecules.

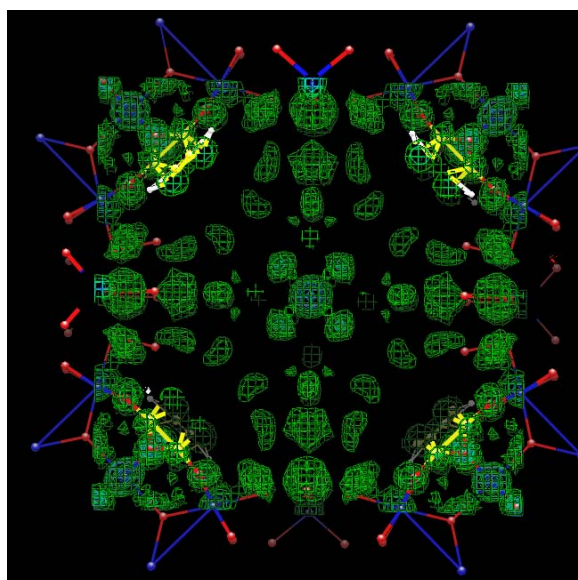


Figure S5. Electron density map of $2F_o - F_c$ at 1-sigma level indicating the position of the porphyrin in the unit cell of **porph@MOM-7**.

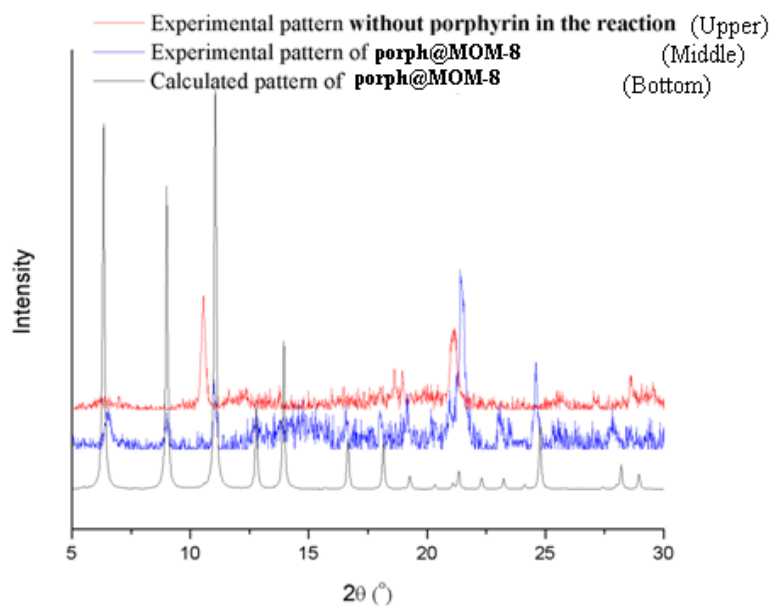


Figure S6. Comparison of experimental and calculated (calculated from **porph@MOM-7**) powder x-ray diffraction patterns of **porph@MOM-8** and the product that was obtained without porphyrin in the reaction.

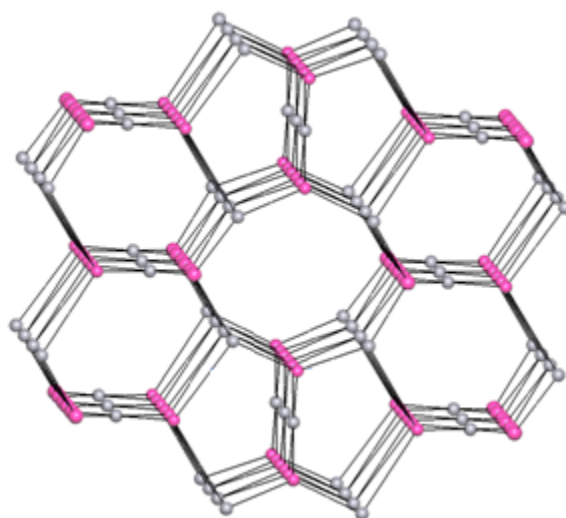


Figure S7. The 3,3,3,4,4,6-c net of **porph@MOM-9**.

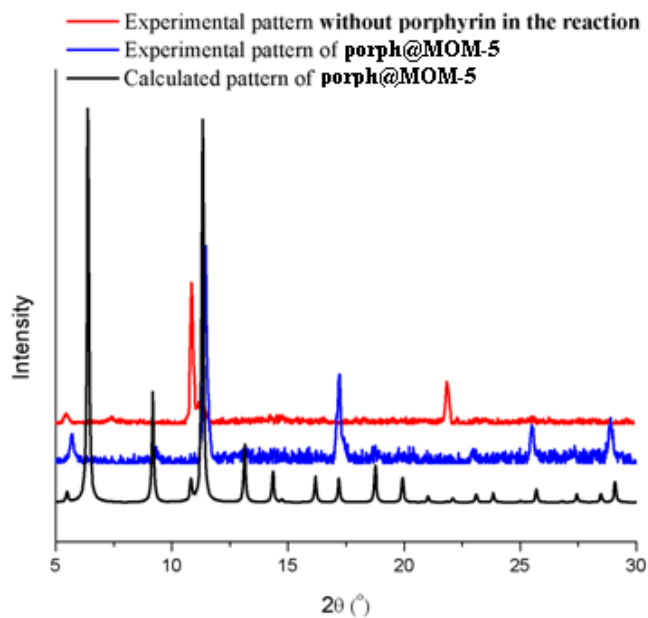


Figure S8. Comparison of experimental and calculated powder x-ray diffraction patterns of **porph@MOM-5** and the product that was obtained without porphyrin in the reaction.

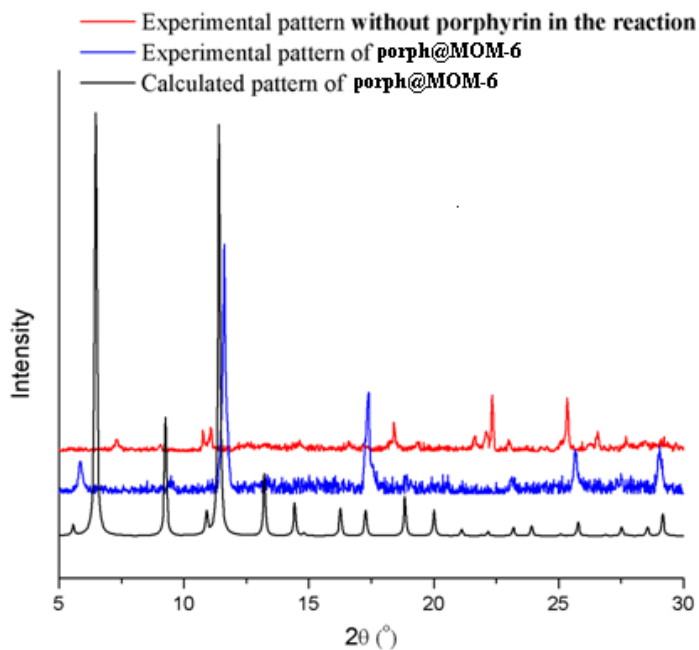


Figure S9. Comparison of experimental and calculated powder x-ray diffraction patterns of **porph@MOM-6** and the product that was obtained without porphyrin in the reaction.

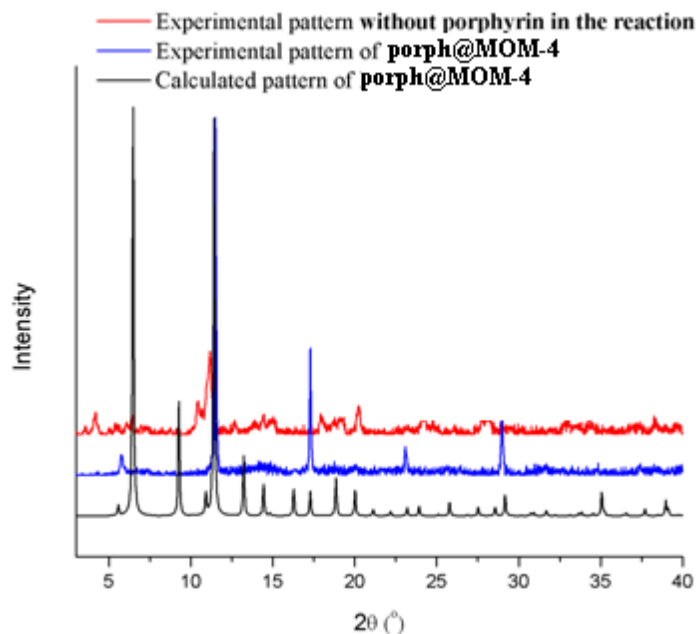


Figure S10. Comparison of experimental and calculated powder x-ray diffraction patterns of **porph@MOM-4** and the product that was obtained without porphyrin in the reaction.

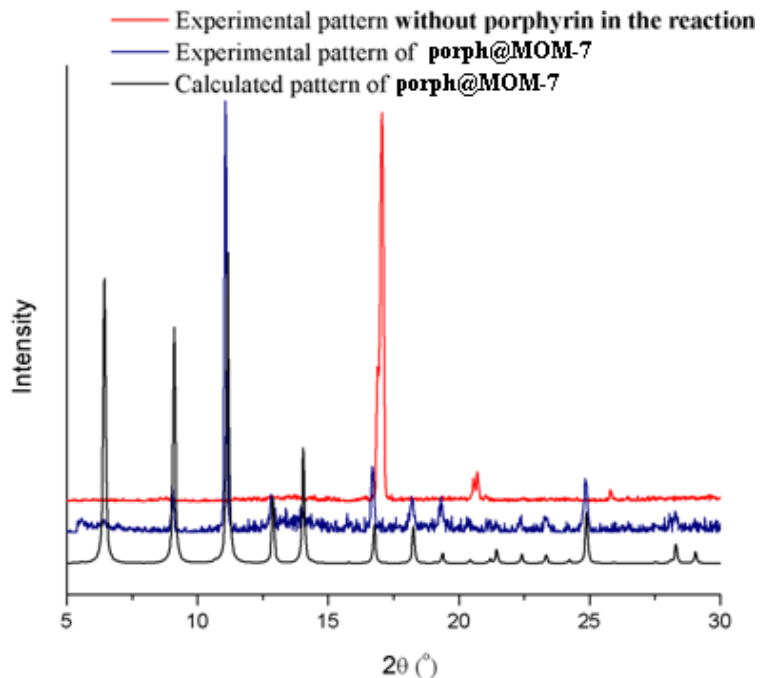


Figure S11. Comparison of experimental and calculated powder x-ray diffraction patterns of **porph@MOM-7** and the product that was obtained without porphyrin in the reaction.

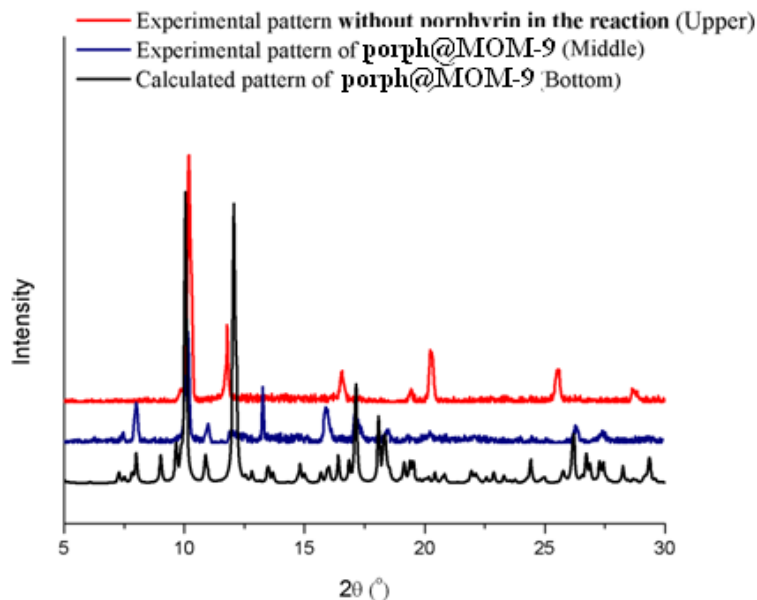


Figure S12. Comparison of experimental and calculated powder x-ray diffraction patterns of **porph@MOM-9** and the product that was obtained without porphyrin in the reaction.

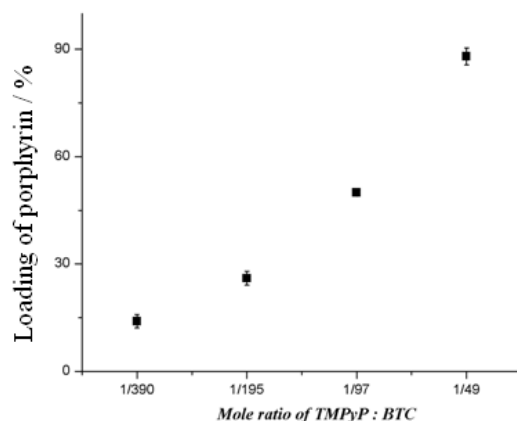


Figure S13. Loading of porphyrin in the middle octahemioctahedral cage varies as the amount of porphyrin added in the reaction. Experimental procedure: A serial of parallel experiments via varying the amount of TMPyP. Crystals were filtered and washed with enough methanol to remove porphines on the crystals' surface. Dissolve the crystals (~4.000 mg, weighted from the TGA machine) into water using a small amount of HCl. The loading of porphyrin was determined by UV-Vis spectrum compared with the standard aqueous solution of FeTMPyP ($\lambda_{\text{max}} = 400 \text{ nm}$).

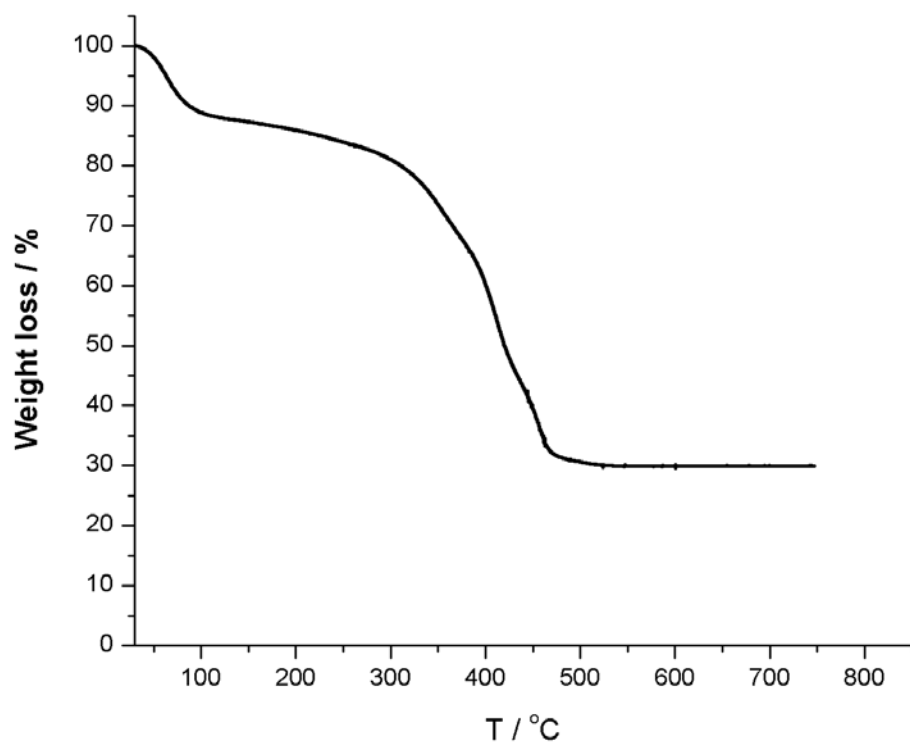


Figure S14. Thermogravimetric analysis of **porph@MOM-4** (Perkin Elmer STA 6000).

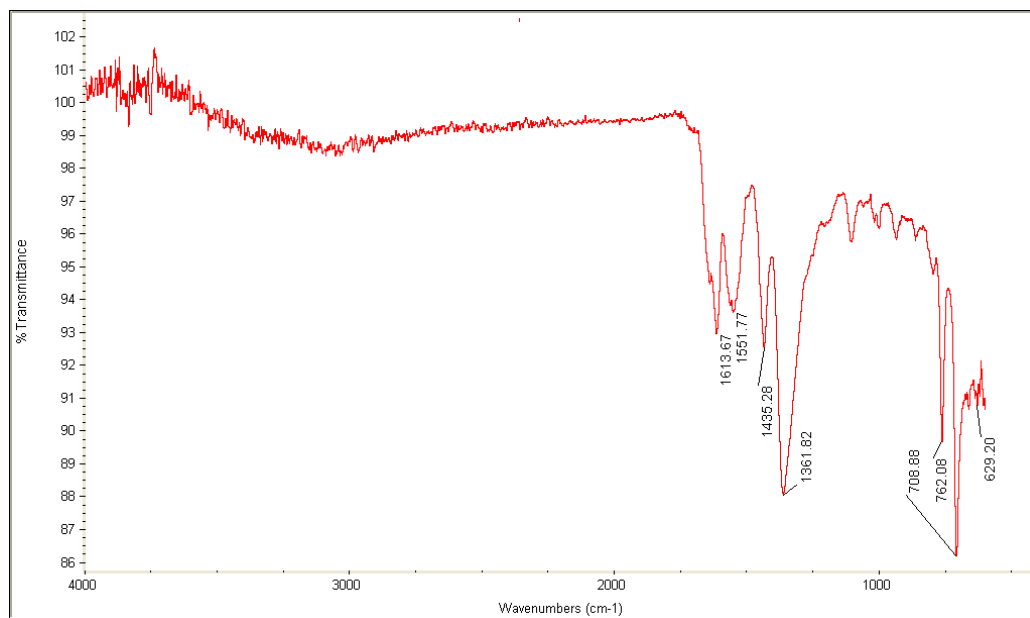


Figure S15. FT-IR of **porph@MOM-4** (Nicolet Avatar 320 FTIR, solid state).

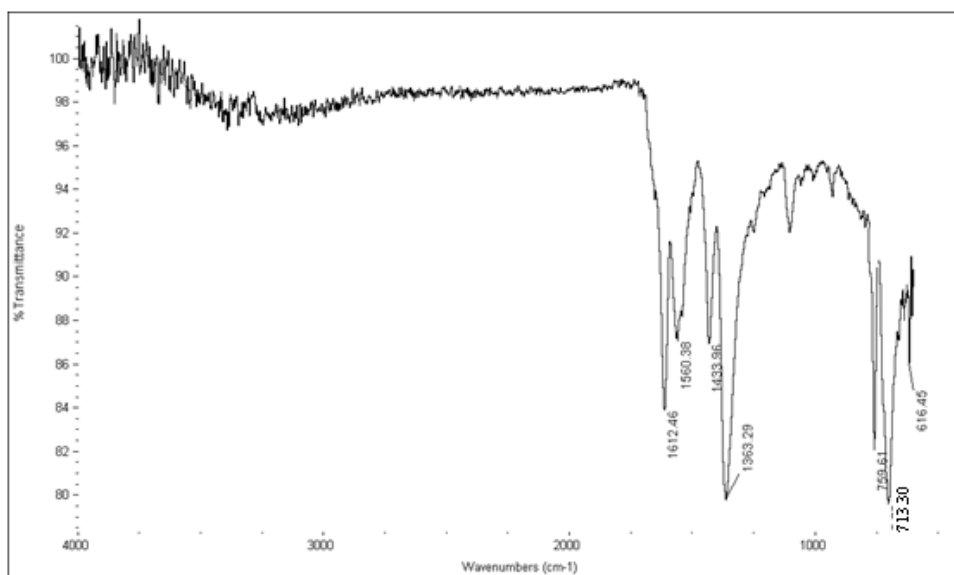


Figure S16. FT-IR of **porph@MOM-5** (Nicolet Avatar 320 FTIR, solid state).

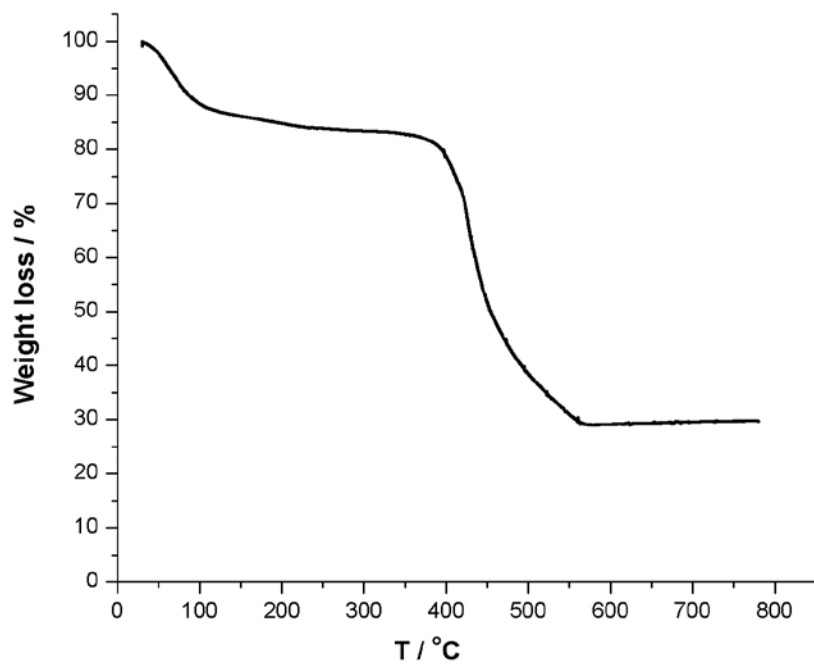


Figure S17. FT-IR of **porph@MOM-5** (Nicolet Avatar 320 FTIR, solid state).

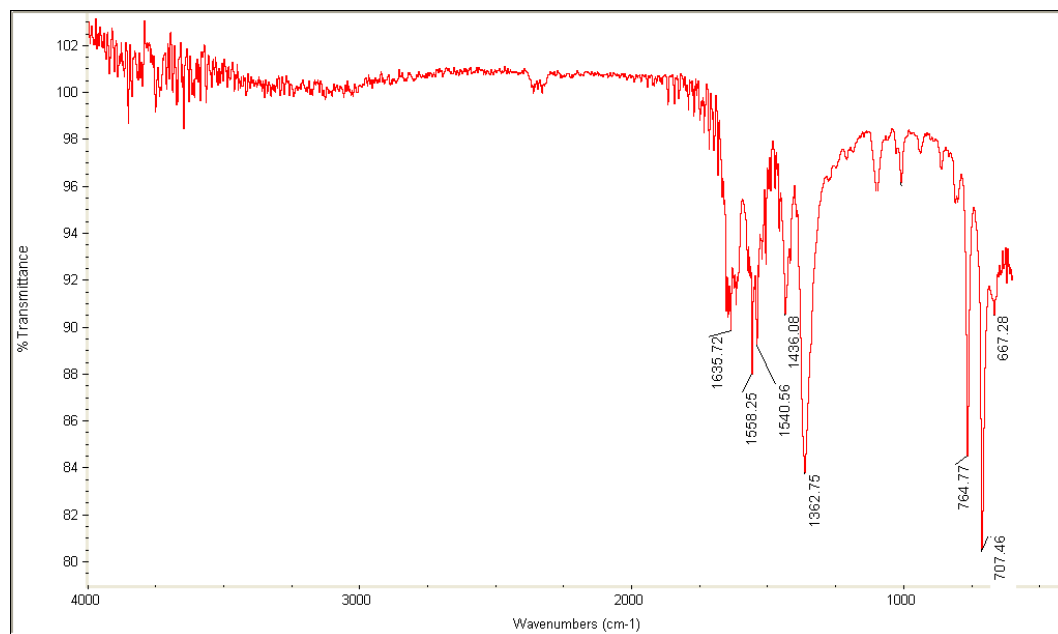


Figure S18. FT-IR of **porph@MOM-6** (Nicolet Avatar 320 FTIR, solid state).

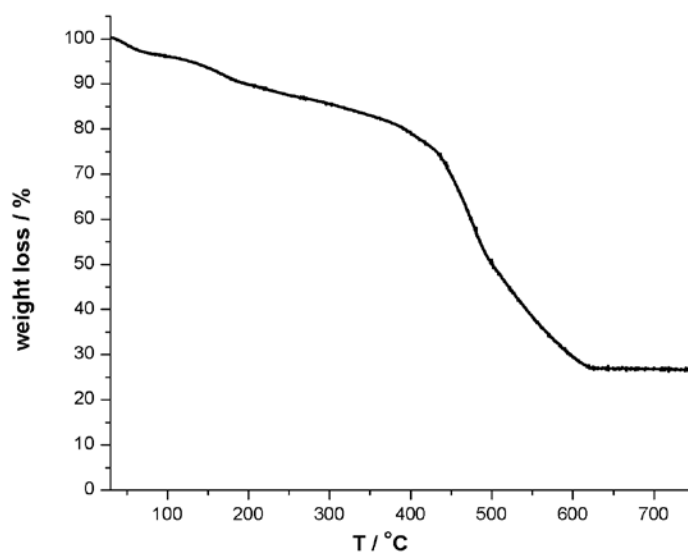


Figure S19. Thermogravimetric analysis of **porph@MOM-6** (Perkin Elmer STA 6000).

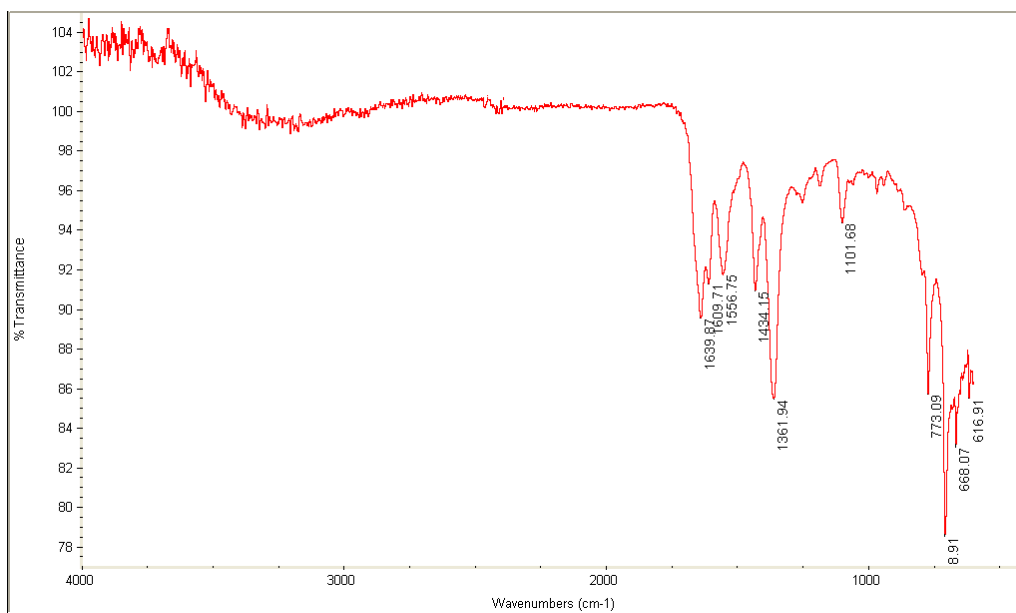


Figure S20. FT-IR of **porph@MOM-7** (Nicolet Avatar 320 FTIR, solid state).

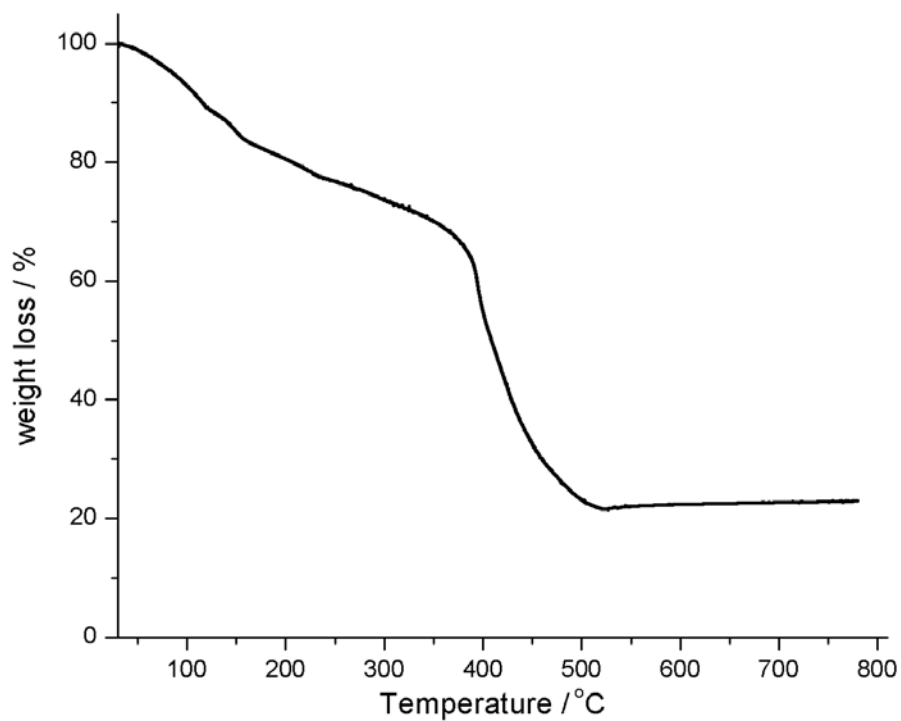


Figure S21. Thermogravimetric analysis of **porph@MOM-7** (Perkin Elmer STA 6000).

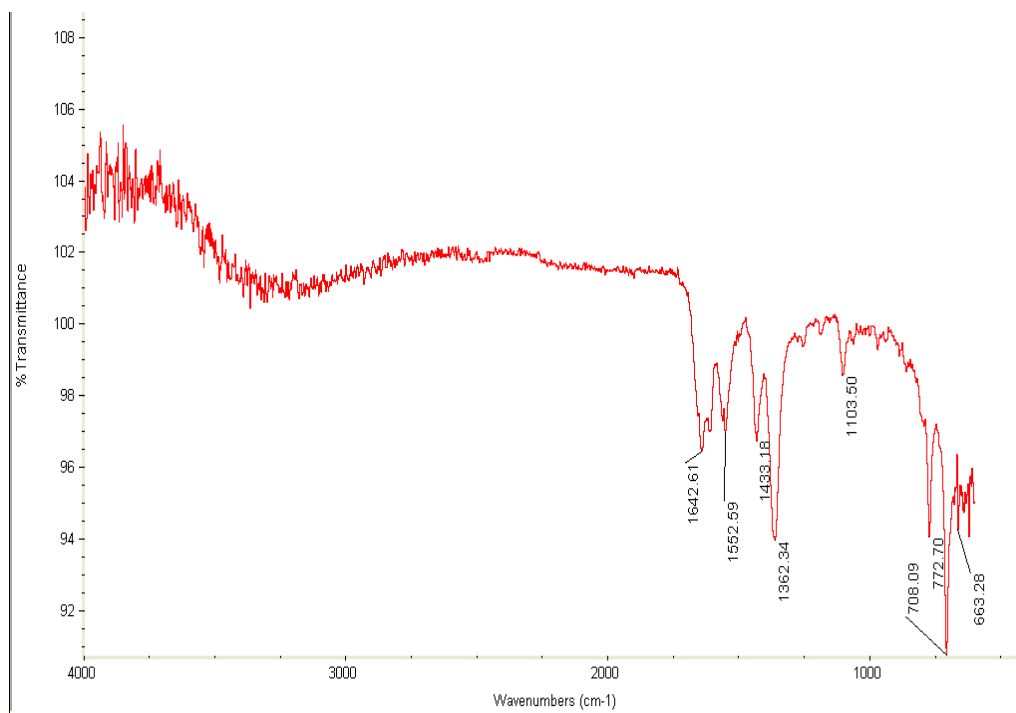


Figure S22. FT-IR of **porph@MOM-8** (Nicolet Avatar 320 FTIR, solid state).

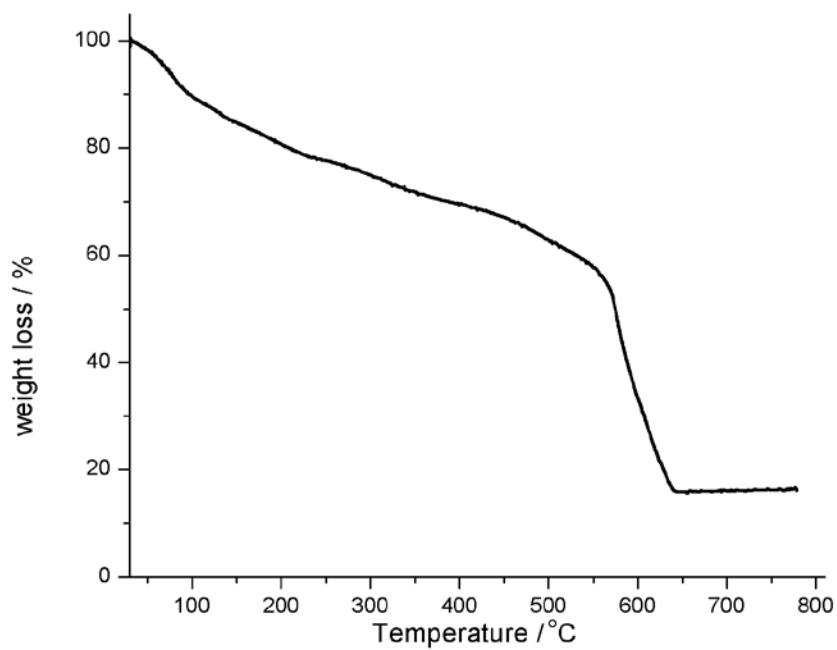


Figure S23. Thermogravimetric analysis of **porph@MOM-8** (Perkin Elmer STA 6000).

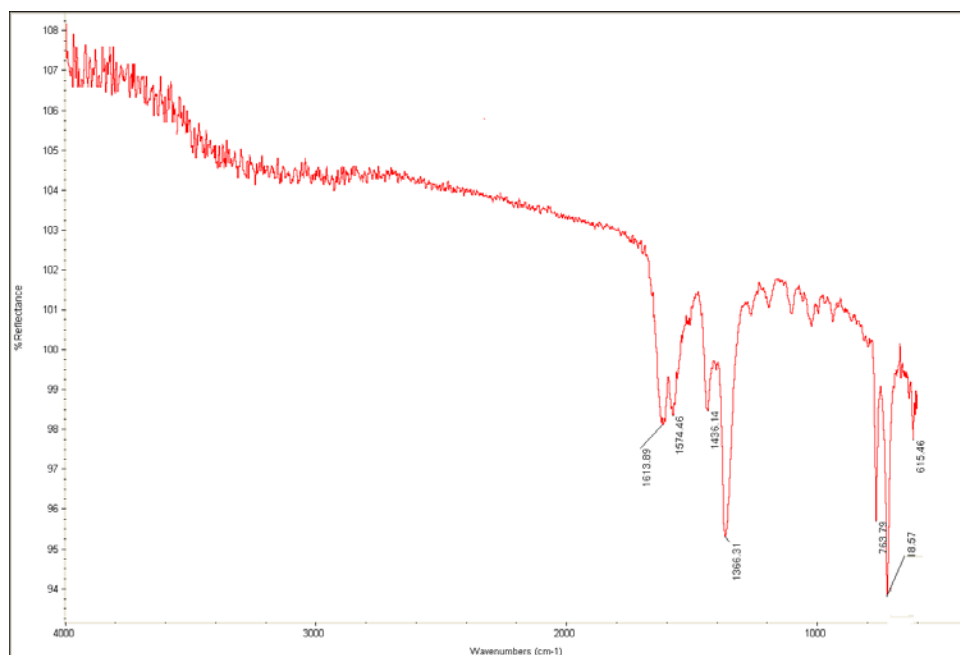


Figure S24. FT-IR of **porph@MOM-9** (Nicolet Avatar 320 FTIR, solid state).

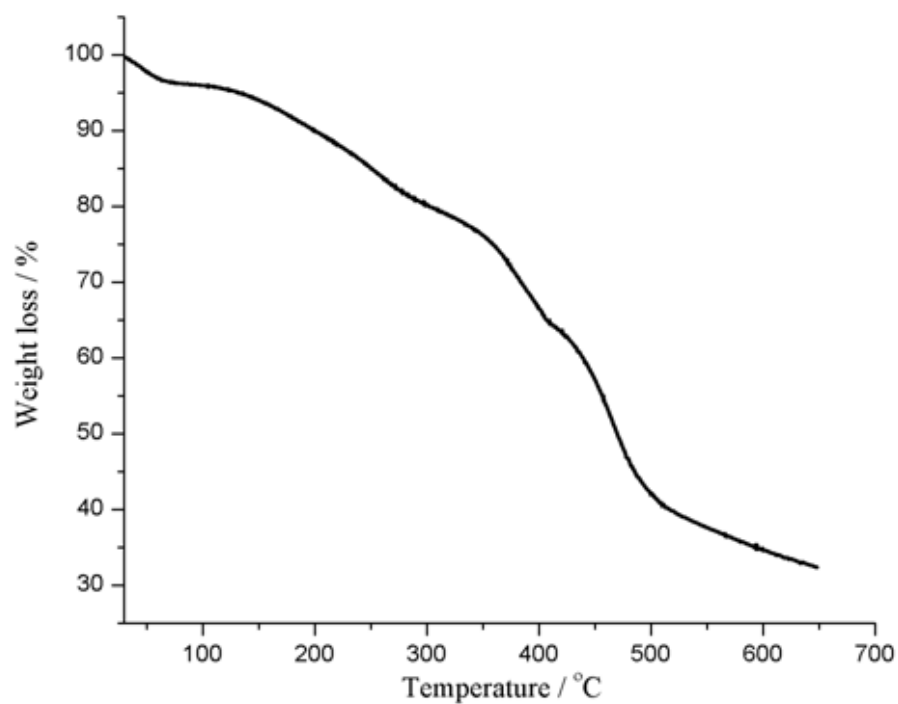


Figure S25. Thermogravimetric analysis of **porph@MOM-9** (Perkin Elmer STA 6000).

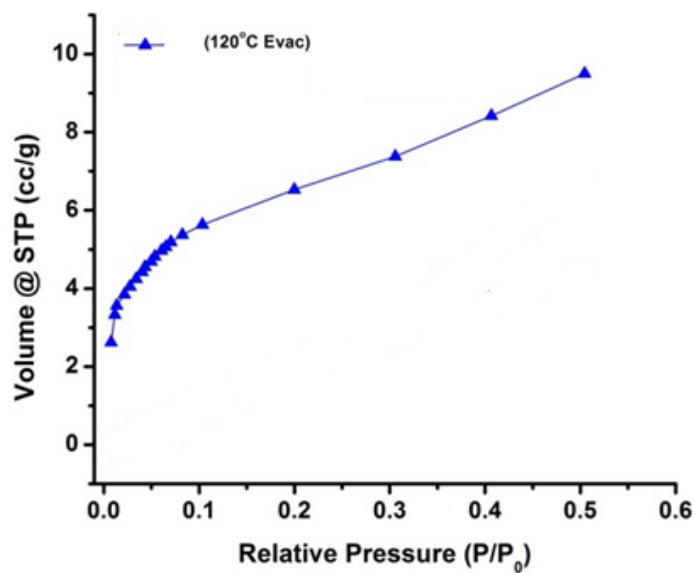


Figure S26. Mini N₂ isotherms for **porph@MOM-7**. Langmuir surface area is 126 m²/g after activation at 120°C.

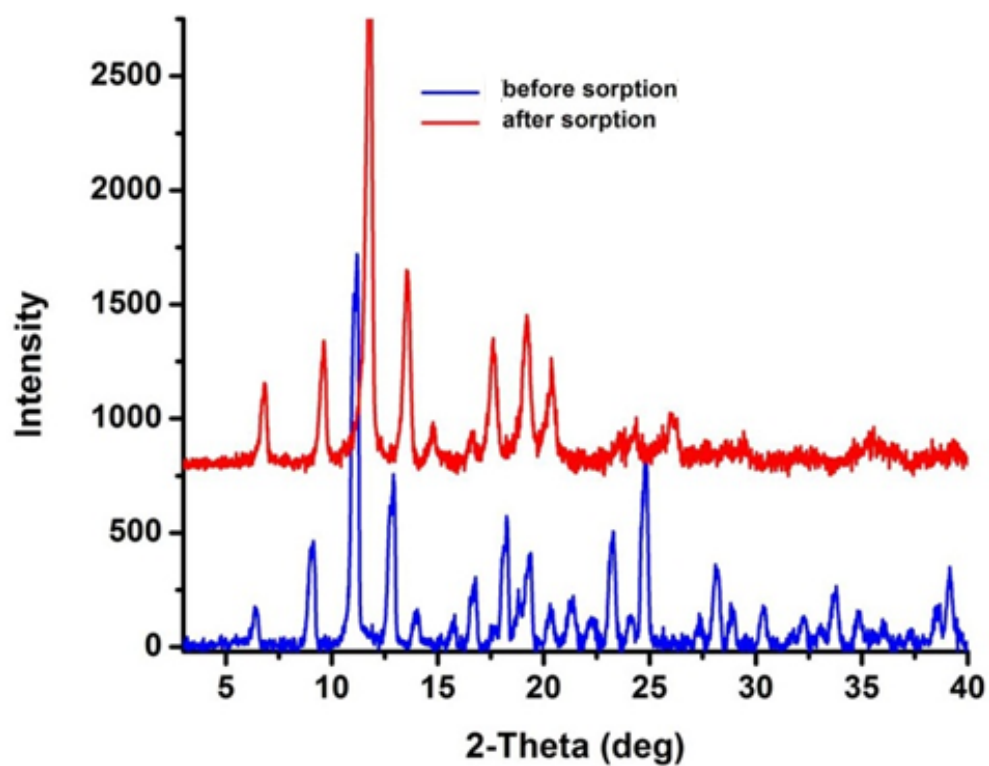


Figure S27. PXRD before and after sorption measurements of **porph@MOM-7**.

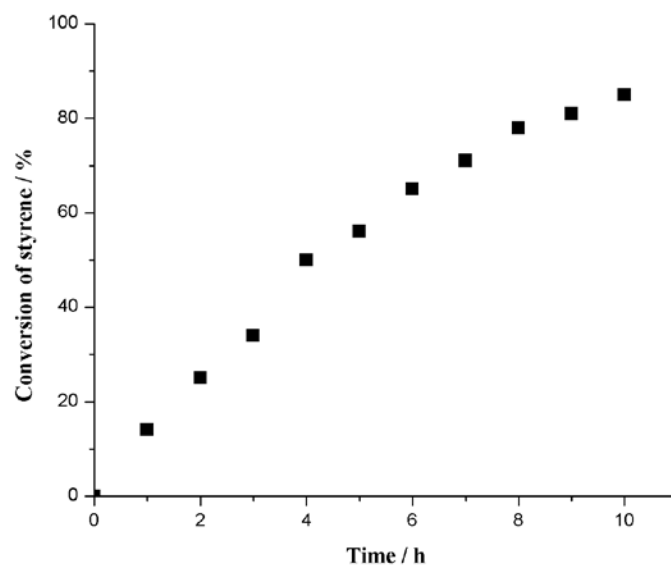


Figure S28. Oxidation of styrene catalyzed by **porph@MOM-4** as measured by GC-MS.

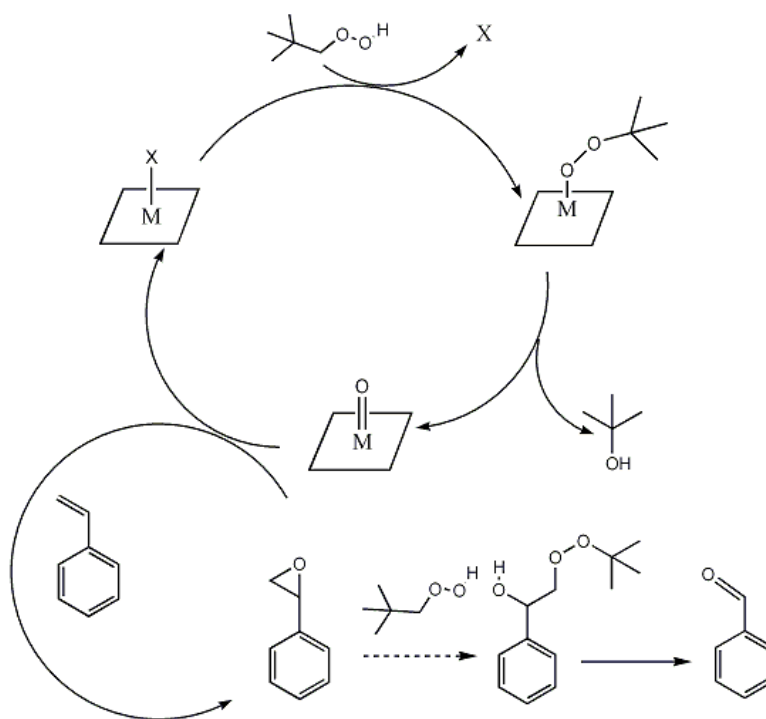


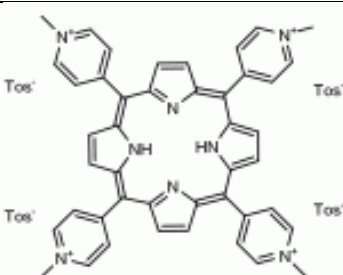
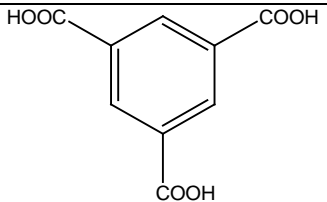
Figure S29. Proposed reaction mechanism for Oxidation of styrene catalyzed by **porph@MOM-4** (M = Mn, Fe, and Co).

Table S1. Catalysis results for **porph@MOM-4**, Fe(III)TMPyP, and control reactions (the same reaction condition without porphyrin).

Styrene				
Catalysts	Conversion	TOF(h ⁻¹)	Selectivity for major products	
			Styrene oxide	Benzaldehyde
porph@MOM-4 (10.0 mg)	85%(10h)	269	30%	57%
Fe(III)TMPyP(1.4mg)	35% (10h)	20	35%	56%
none	<7% (10h)			
Benzoic acid and 1-phenylethanone are the major by-products in this reaction.				
Trans-stilbene				
Catalysts	Conversion	TOF(h ⁻¹)	Selectivity for major products	
			stilbene oxide	Benzaldehyde
porph@MOM-4 (10.0 mg)	40% (10h)	126	70%	28%
Fe(III)TMPyP(1.4mg)	34% (10h)	18	50%	48%
none	<2% (10h)			
Benzoic acid is the major by-product in this reaction.				
Triphenylethylene				
Catalysts	Conversion	TOF(h ⁻¹)	Selectivity for major products	
			Diphenylmeth -anone	Benzaldehyde
porph@MOM-4 (10.0 mg)	5% (10h)	15	49%	18%
Fe(III)TMPyP(1.4mg)	14% (10h)	8	48%	11%

none	<4% (10h)	
Benzoic acid and benzoic acid butyl ester are the major by-products in this reaction.		

Substrate conversion (%) = $\frac{\text{Substrate converted (moles)}}{\text{Substrate used (moles)}} \times 100$, Product selectivity (%) = $\frac{\text{Product formed (moles)}}{\text{Substrate converted (moles)}} \times 100$

Table S2. A. Reaction with porphyrin as template		
<p>FeCl₂</p>  <p>TMPyP</p>  <p>BTC</p>	<p>3.0 mL DMF</p> <p>0.5 mL H₂O</p> <p>85°C</p> <p>➔</p>	<p>porph@MOM-4</p> <p>[Fe₁₂(BTC)₈(S)₁₂]Cl₆·xFeTMPyPCL₅</p> <p>(S = H₂O or DMF, x is depending upon the relative amount of porphyrin used during synthesis)</p> <p>Crystal system = Cubic</p> <p>Space group = <i>Fm-3m</i></p> <p>a = 26.5717(17) Å,</p> <p>V = 18761(2) Å³</p> <p>This compound is isostructural with HKUST-1-Cu which was previously report by Williams et al.:</p> <p>Chui, S. S.-Y., Lo, S. M.-F., Charmant, J. P. H., Guy Orpen, A. & Williams, I. D. A chemically functionalizable nanoporous material [Cu₃(TMA)₂(H₂O)₃]_n. <i>Science</i> 283, 1148–1150 (1999).</p>
B. Reaction without porphyrin		
		Yellow precipitate of a compound that

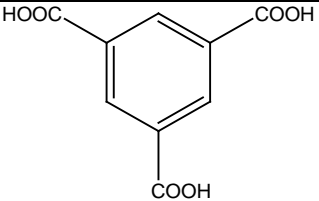
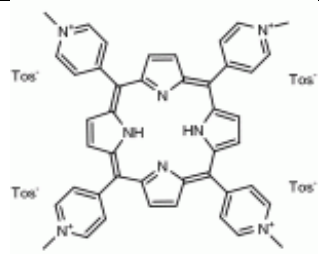
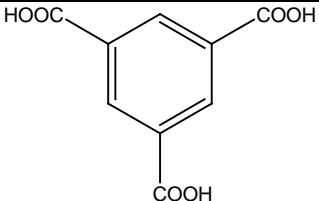
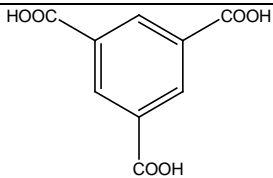
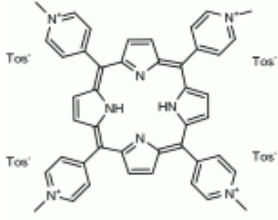
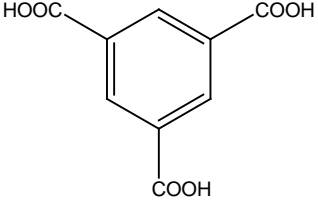

FeCl_2	3.0 mL DMF 0.5 mL H ₂ O 85°C	exhibits a different powder x-ray diffraction pattern to that of porph@MOM-4
 BTC	➔	

Table S3. A. Reaction with porphyrin as template

CoCl_2		porph@MOM-5 $[\text{Co}_{12}(\text{BTC})_8(\text{S})_{12}] \cdot x\text{CoTMPyP}\text{Cl}_4$ (S = solvent, x is depending upon the relative amount of porphyrin used during synthesis) Crystal system = Cubic Space group = <i>Fm-3m</i> $a = 26.4292(11) \text{ \AA}$, $V = 18460.9(13) \text{ \AA}^3$
 TMPyP	3.0 mL DMF 0.5 mL H ₂ O 85°C	
 BTC	➔	This compound is isostructural with HKUST-1-Cu which was previously report by Williams et al.: Chui, S. S.-Y., Lo, S. M.-F., Charmant, J. P. H., Guy Orpen, A. & Williams, I. D. A chemically functionalizable nanoporous material

		$[\text{Cu}_3(\text{TMA})_2(\text{H}_2\text{O})_3]_n$. <i>Science</i> 283 , 1148–1150 (1999).
B. Reaction without porphyrin		
<p>CoCl_2</p>  <p>BTC</p>	<p>3.0 mL DMF 0.5 mL H_2O 85°C</p> <p>→</p>	<p>$[\text{Co}_6(\text{HCOO})(\text{BTC})_2(\text{DMF})_6]_n$</p> <p>Crystal system = Trigonal</p> <p>Space group = $P-3$</p> <p>$a = 13.975(2) \text{ \AA}$ $c = 8.165(1) \text{ \AA}$, $V = 1380.990 \text{ \AA}^3$</p> <p>This product was previously reported by Xu et al.: He, J., Zhang, Y., Pan, Q., Yu, J., Ding, H. & Xu, R. Three metal-organic frameworks prepared from mixed solvents of DMF and HAc. <i>Microporous Mesoporous Mater.</i> 90, 145-152 (2006).</p>
Table S4. A. Reaction with porphyrin as template		
<p>MnCl_2</p>  <p>TMPyP</p>	<p>3.0 mL DMF 0.5 mL H_2O 85°C</p>	<p>porph@MOM-6</p> <p>$[\text{Mn}_{12}(\text{BTC})_8(\text{S})_{12}] \cdot x\text{MnTMPyP}\text{Cl}_5$</p> <p>(S = H_2O or DMF, x is depending upon the relative amount of porphyrin used during synthesis)</p> <p>Crystal system = Cubic</p> <p>Space group = $Fm-3m$</p> <p>$a = 26.597(2) \text{ \AA}$,</p>

 <p style="text-align: center;">BTC</p>		<p>$V = 18460.9(13) \text{ \AA}^3$</p> <p>This compound is isostructural with HKUST-1-Cu which was previously report by Williams et al.: Chui, S. S.-Y., Lo, S. M.-F., Charmant, J. P. H., Guy Orpen, A. & Williams, I. D. A chemically functionalizable nanoporous material $[\text{Cu}_3(\text{TMA})_2(\text{H}_2\text{O})_3]_n$. <i>Science</i> 283, 1148–1150 (1999).</p>
--	---	--

B. Reaction without porphyrin

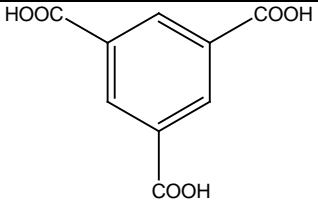

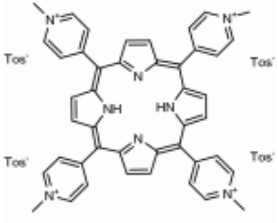
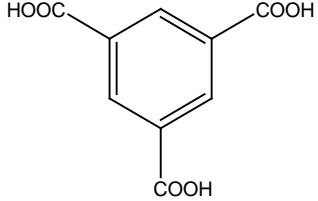
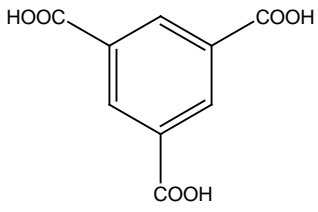
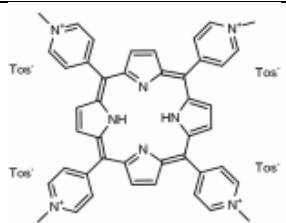
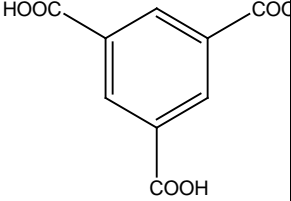
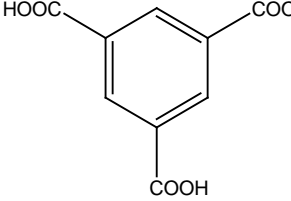
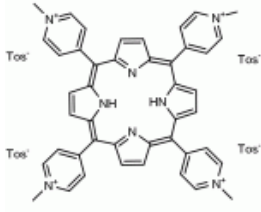
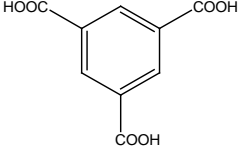
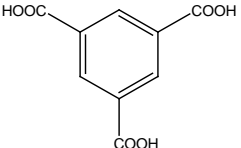
<p style="text-align: center;">MnCl_2</p> 	<p>3.0 mL DMF</p> <p>0.5 mL H_2O</p> <p>85°C</p> 	<p>$[\text{Mn}_6(\text{HCOO})(\text{BTC})_2(\text{DMF})_6]_n$</p> <p>Crystal system = Trigonal</p> <p>Space group = $P-3$</p> <p>$a = 13.90 \text{ \AA}$</p> <p>$c = 8.11 \text{ \AA}$,</p> <p>$V = 1434.454 \text{ \AA}^3$</p> <p>This product was previously reported by Kitagawa et al.: Chen, J., Ohba, M. & Kitagawa, S. Two New Coordination Polymers Based on Hexanuclear Metal Cluster Cores. <i>Chem. Lett.</i> 35, 526-527 (2006).</p>
--	---	---

Table S5.A. Reaction with porphyrin as template

<p>$\text{Ni}(\text{OAc})_2$</p>		<p>porph@MOM-7</p>
---	--	---------------------------

 <p>TMPyP</p>	<p>2.0 mL DMF</p> <p>0.4 mL H₂O</p> <p>85°C</p> <p>➔</p>	<p>$[\text{Ni}_{10}(\text{BTC})_8(\text{S})_{24}] \cdot x\text{NiTMPyP} \cdot (\text{H}_3\text{O})_{(4-4x)}$ (S = solvent, x is depending upon the relative amount of porphyrin used during synthesis)</p> <p>Crystal system = Cubic</p> <p>Space group = <i>Fm-3m</i></p> <p>$a = 27.478(2) \text{ \AA}$,</p> <p>$V = 20747(3) \text{ \AA}^3$</p>
 <p>BTC</p>		
B. Reaction without porphyrin		
<p>Ni(OAC)₂</p> 	<p>2.0 mL DMF</p> <p>0.4 mL H₂O</p> <p>85°C</p> <p>➔</p>	<p>Prismatic light green crystals of a compound that exhibits a different powder x-ray diffraction pattern to that of porph@MOM-7 were obtained.</p>
Table S6. A. Reaction with porphyrin as template		
<p>Mg(OAC)₂</p>  <p>TMPyP</p>	<p>2.0 mL DMF</p> <p>0.4 mL H₂O</p> <p>85°C</p>	<p>porph@MOM-8</p> <p>$[\text{Ni}_{10}(\text{BTC})_8(\text{S})_{24}] \cdot x\text{NiTMPyP} \cdot (\text{H}_3\text{O})_{(4-4x)}$ (S = H₂O or DMF, x is depending upon the relative amount of porphyrin used during synthesis)</p>

 <p>BTC</p>	<p>→</p>	
B. Reaction without porphyrin		
 <p>Mg(OAc)₂</p>	<p>2.0 mL DMF 0.4 mL H₂O 85°C</p> <p>→</p>	<p>Prismatic colorless crystals of a compound that exhibits a different powder x-ray diffraction pattern to that of porph@MOM-8 were obtained.</p>
Table S7.A. Reaction with porphyrin as template		
<p>Zn(NO₃)₂</p>  <p>TMPyP</p>	<p>3.0 mL DMA 0.5 mL H₂O 85°C</p>	<p>porph@MOM-9 [Zn₁₈(OH)₄(BTC)₁₂(S)₁₅]·xZnTMPyP·H₃O_(4-4x) (S = solvent, x is depending upon the relative amount of porphyrin used during synthesis)</p>

 <p>BTC</p>	<p>➔</p>	<p>Crystal system = Orthorhombic</p> <p>Space group = <i>Cmmm</i></p> <p>$a = 19.653(3) \text{ \AA}$; $b = 44.127(6) \text{ \AA}$</p> <p>$c = 14.543(2) \text{ \AA}$; $V = 12612(3) \text{ \AA}^3$</p>
<p>B. Reaction without porphyrin</p>		
<p>$\text{Zn}(\text{NO}_3)_2$</p> 	<p>3.0 mL DMA</p> <p>0.5 mL H₂O</p> <p>85°C</p> <p>➔</p>	<p>Crystal system = Cubic</p> <p>$a = 15.350(5) \text{ \AA}$; $V = 3616.9(18) \text{ \AA}^3$</p> <p>Triangular shaped colorless crystals of a compound that exhibits a different PXRD pattern to that of porph@MOM-9 were obtained.</p>